

1 **The exchange of dissolved nutrients between water column and substrate pore-water due to**
2 **hydrodynamic adjustment at seagrass meadow edges: A flume study**

3

4 A. Adhitya^{1*,5}, A.M. Folkard², L. L. Govers^{3,4,5}, M.M. van Katwijk³, H. H. de Iongh^{6,7}, P.M.J.

5 Herman¹, T.J. Bouma^{1*}

6

7 Running Head: Seagrass Porewater Exchange Hydrodynamic

8

9

10

11



12 ¹Royal Netherlands Institute for Sea Research (NIOZ) P.O. Box 140, 4400AC Yerseke, The Netherlands.

13 Corresponding Author: Tjeerd.Bouma@NIOZ.NL and Achmad.Adhitya@NIOZ.NL

14 ²Lancaster Environment Centre, University of Lancaster, Lancaster LA1 4YQ, United Kingdom

15 ³ Department of Environmental Science, Institute for Water and Wetland Research, Radboud University
16 Nijmegen, Faculty of Science, P.O. Box 9010, 6500 GL Nijmegen, The Netherlands

17 ⁴Department of Aquatic Ecology and Environmental Biology, Institute for Water and Wetland Research,
18 Radboud University Nijmegen, Faculty of Science, P.O. Box 9010, 6500 GL Nijmegen, The Netherlands

19 ⁵Conservation Ecology Group, Groningen Institute for Evolutionary Life Sciences, University of
20 Groningen, Post Office Box 11103, 9700 CC Groningen, The Netherlands

21 ⁶Institute of Environmental Sciences, CML/Conservation Biology, Van Steenis gebouw
22 Einsteinweg P.O. BOX 22333 CC Leiden, The Netherlands

23 ⁷Department Evolutionary Biology, Groenenbergerlaan 17, 2020, Antwerpen Belgium

24

25 **Acknowledgements**

26 This work was supported by a NWO WOTRO host fellowship for transfer of knowledge,
27 WOTRO-WT-84-644. We thank Jos van Soelen, Bas Koutstaal, and Louie Haazen for invaluable
28 technical assistance.

29

30

31

32

33

34

35

36

37

38

39

40

41

42

43

44

45

46

47 **ABSTRACT**

48 Seagrasses need dissolved nutrients to maintain their productivity through uptake processes, from
49 substrate pore-water via their roots and/or from water column via their leaves. Here, we present the
50 first study of exchanges of dissolved nutrients between pore water and the water column in the vicinity
51 of seagrass canopies. We address the following research questions, using a laboratory flume
52 experiment: 1) How does solute exchange between open water and substrate pore water vary spatially
53 within seagrass patches? 2) How does seagrass leaf length affect this solute exchange? 3) How does the
54 measured rate of solute exchange compare with seagrasses' rates of uptake of dissolved nutrients? Our
55 results indicate that solute intrusion from open water into substrate pore water is highest in the area
56 around seagrass patches' leading edges, where flow deceleration is strongest, and decreases
57 approximately linearly with downstream distance into the patch. The decrease in measured flow speed
58 in the canopy fits well the predictions of previously reported models of arrays of rigid obstacles. The
59 length of the region in which the concentration of solute that has infiltrated into the substrate at the
60 upstream end of the seagrass patches is similar to the length scale predicted from model estimates of
61 infiltration rate (based on the substrate permeability) and the length of time over 24-hour runs. We
62 conclude that the mechanism we identify only pertains near canopy edges, and therefore that other
63 mechanisms must govern nutrient supply in the interior of seagrass meadows.

64

65

66

67

68

69

70

71 **Introduction**

72 Seagrass meadows are highly productive ecosystems that provide important services
73 such as offering nursery and other habitats to a wide range of marine species (Kennedy et al.,
74 2010; Short et al., 2011; Cullen-Unsworth et al., 2013), contributing to shoreline protection by
75 reducing erosion (Hendriks et al., 2007; Christiansen et al., 2013) and attenuating wave and
76 current energy (Pujol and Nepf, 2012; Paul et al., 2012). In recent decades, seagrass meadows
77 have decreased globally at an alarming rate (Cambridge et al., 1986; Morris and Virnstein, 2004;
78 Waycott et al., 2009). This decline has often been linked to problems with water quality: either
79 enhanced turbidity (van der Heide et al., 2007, Carr et al., 2010) or hypertrophic nutrient
80 concentrations causing algae blooms (Gacia and Duarte, 2001; Apostolaki et al., 2010). In
81 contrast to our knowledge about threats associated with high nutrient concentrations, we have
82 a poor understanding of how seagrasses can flourish in the low nutrient (oligotrophic)
83 environments in which they are often found, particularly in many tropical regions.

84 Contrary to many terrestrial macrophytes, seagrasses are poor at resorbing nitrogen
85 from senescing leaves, resulting in high N-losses due to leaf detachment (Stapel et al., 1997;
86 Romero et al., 2006). The high productivity and leaf-loss of seagrasses result in a nutrient
87 paradox (Hemminga et al., 1999; Reyes and Sanson, 2001): How can seagrasses maintain their
88 productivity if so much of their nutrients is lost via senescing leaves? Possible solutions to this
89 paradox are that the leaves degrade within the meadow, enabling re-uptake of their nutrients
90 by the seagrass (Peduzzi and Herndl, 1991; Apostolaki et al., 2010); trapped suspended particles
91 may similarly contribute (Hendriks et al., 2007; Duarte et al., 2011; Kennedy et al., 2010) or
92 seagrasses can take up dissolved organic nitrogen (DON) from sources within the bed sediment

93 (Barron et al., 2006, Vonk et al., 2008, Van England et al., 2011). Whereas these latter studies
94 show that DON may provide an important N source to seagrass roots, we lack insight into how
95 DON, or suspended matter, enters the substrate beneath seagrass meadows.

96 For bare, permeable, sandy sediment substrates, several studies have shown high rates
97 of water exchange between the open water column above the substrate and the pore water
98 within it, which may cause biological and chemical modifications of the pore water via
99 advection of suspended or dissolved matter (Huettel and Gust, 1992; Huettel and Rusch, 2000).
100 Such fluxes are generally caused by pressure gradients, which may be due to wave propagation
101 causing pressure oscillations at the sediment surface (Webb and Theodor, 1972; Shum, 1992;
102 Precht and Huettel, 2004) or to currents' interactions with seabed topography (Huettel and
103 Webster, 2001). For example, a local vertical pressure gradient of 100 Pa m^{-1} , caused by flow
104 encountering a small rise in the bed, is enough to force water several centimeters into the
105 sediment and draw pore water from more than 0.1 m beneath the sediment surface into the
106 water column (Huettel et al., 1998).

107 If advective exchange between water column and pore water (referred to hereinafter
108 as "pore water exchange") also occurs within seagrass meadows, it could provide an important
109 supply of DON to seagrass roots, which are particularly good at taking up DON (Evrard et al.,
110 2005; Vonk et al., 2008; Van England et al., 2011). Little is known about this phenomenon in the
111 presence of seagrass. Laboratory flume experiments have been reported that have provided
112 models of flow adjustments at the upstream end of vegetation(-mimic) canopies (Folkard 2005;
113 Tanino and Nepf, 2008; Chen et al., 2013). The general pattern observed in these experiments is
114 that, on encountering such a canopy, the flow adjusts to the canopy's presence such that part

115 of it is deflected upwards and travels at accelerated speeds over the top of the canopy, and
116 part travels at decelerated speeds through the canopy. However, there is also a third possible
117 flow path – just as the flow can be deflected over the canopy, it can also be deflected beneath
118 it, into the permeable substrate. This mechanism is analogous to the enhancement of
119 infiltration by pressure gradients around seabed topography discussed by Huettel et al. (1998)
120 and would cause changes in the pore water exchange rate: we would expect enhanced
121 infiltration from the open water into the substrate while the in-canopy flow decelerates as a
122 result of the presence of the canopy. Although other laboratory experimental studies have
123 investigated the influence of seagrass canopy structure on solute uptake rates from the open
124 water (Thomas et al., 2000; Morris et al., 2008), this hydrodynamic mechanism of enhanced
125 pore water exchange, which would be expected to affect nutrient supply to seagrass roots, has
126 not previously been investigated. Hence, here we used laboratory flume experiments to
127 elucidate and quantify pore water exchange in the presence of patches of seagrass mimics.
128 Since the geometric configuration of the seagrass canopy might be expected to be a primary
129 factor in determining the magnitude of this phenomenon, we investigated the influence on it of
130 different canopy heights (leaf lengths).

131

132 **Material and Methods**

133 To measure the effect of seagrass canopies on pore water exchange in a spatially explicit
134 way, we carried out experiments in a race track laboratory flume at the Royal Netherlands
135 Institute for Sea Research (NIOZ) in Yerseke (Fig. 1a; details in Bouma et al. 2009). Coral sand
136 collected from a natural, oligotrophic seagrass meadow in Indonesia (median grain size $d_{50} = 5.8$

137 $\times 10^{-4}$ m; permeability 1.6×10^{-11} m²) was placed into the test section of the flume (2 m long x
138 0.6 m wide), which had a false floor to a depth of 0.15 mm, such that the top of the sand layer
139 was flush with the flume bed. The whole flume was then filled with fresh water to a height $H =$
140 0.40 m above the sand surface. We measured the pore water content of the sand used in the
141 flume test section by taking replicate samples of 0.5 l of the sand, placing them in a 1 l
142 graduated cylinder and covering them with water. We took the volume indicated by the surface
143 of the sand in the cylinder as the combined volume of the sand and pore water, and subtracted
144 the 0.5 l volume of the sand from this to give the pore water volume. The water volume thus
145 measured was 0.189 ± 0.004 l (mean + 1 sd; $n = 5$), giving a porosity (water:total volume ratio)
146 of 0.274 ± 0.004 (volumetric sand: water ratio 2.65 ± 0.05 , volumetric water:sand ratio $0.378 +$
147 0.006).

148 To simulate the seagrass, we used polyethylene mimics, a generally accepted approach
149 in flume studies of hydrodynamic processes within seagrass beds (e.g., Nepf & Vivoni, 2000;
150 Folkard, 2005; Bouma et al., 2009). The polyethylene used had modulus of elasticity $E = 1.09 \pm$
151 0.425×10^7 Nm⁻² ($N = 6$). The design of our mimics was based on field observations of *Thalassia*
152 *hemprichii*. at the same location in Indonesia from where the sediment was taken. Two sets of
153 mimics were created. The first (the “long-leaved” mimics) consisted of four leaves per shoot,
154 each leaf being 0.14 m long, 0.01 m wide and 0.0001 m thick. These leaves were attached to
155 0.08 m-long sheaths that were inserted into the coral sand in the flume, so that the top of the
156 sheath was level with the sand surface, and the leaves protruded above the sand into the water
157 column. The second (the “short-leaved” mimics) consisted of two leaves per shoot, each being
158 0.1 m long, 0.01 m wide and 0.0001 m thick. These leaves were attached to 0.05 m-long

159 sheaths, which were similarly inserted into the sand such that their tops were flush with the
160 sand surface. These sheaths clearly simplify the below-ground structure of seagrass roots and
161 rhizome systems, but we assume that this does not affect our ability to elucidate the
162 mechanism of pore water exchange. In both cases, a 1 m long patch of plant mimics with a
163 density of 722 shoots m^{-2} (c.f. shoot densities observed in natural *Thalassia* meadows of 48–
164 1888 shoots m^{-2} with uniform spatial configuration, Lewis, 1984; Tomasko and Lapointe, 1991;
165 Barry, 2013), which filled the whole 0.6 m width of the flume, was fabricated and placed in the
166 flume test section, leaving 0.5 m of bare sand both upstream and downstream (Fig. 1b). Since
167 the upstream adjustment of the flow occurs over a distance comparable to the meadow height
168 (i.e. at most 0.14 m for the long leaves, and 0.1 m for the short leaves) this length of bare sand
169 should capture any variations in solute exchange due to such flow adjustments (Folkard,
170 unpublished data). We did not test a control case with no seagrass, as we assumed that there
171 would be no systematic variation in solute exchange in such a case, and that the rate of
172 exchange would be comparable to that measured 0.25 m upstream of the canopy in these
173 experiments, due to the lack of variation in bottom conditions. Along-flume locations are
174 identified using the coordinate x , where $x = 0$ is the upstream end of the patch (positive
175 downstream), and vertical locations using the coordinate z , where $z = 0$ is the surface of the
176 sand (positive upwards). The penetration of nutrients into the sediment was detected using
177 bromide as a conservative proxy tracer. Tracers are commonly used for characterizing flows in
178 surface waters, and estimating groundwater discharges (Replogle et. al., 1968; Finker and
179 Gilley, 1986). Bromide is suitable for usage in surface water (Smith and Davis., 1974; Gilley et.
180 al., 1990), and for determining hydraulic parameters both in the field (Owens, 1985; Lin et. al.,

181 2003), and laboratory (Glud et. al., 1994; Foster et. al., 1999; Rasheed et. al., 2003). Here,
182 bromide was added into the surface water at a concentration $[\text{Br}^-]_t$ of 0.1 kg m^{-3} .

183 A current with a mean speed of 0.3 m s^{-1} was passed around the flume, representing
184 typical hydrodynamic conditions observed in shallow seagrass meadows (e.g. Palmer, 1988;
185 Verduin and Backhaus, 2000). After 24 hours exposure of the sediment substrate to the flow of
186 this bromide-seeded open water, cores of the substrate were extracted to determine the
187 amount of bromide that had penetrated into them. The 24-hour period was chosen to ensure
188 that the bromide was well-mixed in the open water column, but was otherwise solely for
189 logistical convenience. The cores were extracted using 0.1 l syringes with their narrow tips cut
190 off, giving cores of approximately 0.05 m in diameter. At each location, the core was extracted
191 by positioning the syringe vertically with the base of the plunger flush with the sediment
192 surface, then pushing the sleeve of the syringe into the sediment whilst keeping the plunger
193 stationary. When the syringe was lifted away, it took with it a core of sediment that retained
194 the relative position of sediment and pore water within itself, which was immediately stored at
195 -20°C . Cores were taken at three random replicate cross-flume locations at each of nine along-
196 flume locations covering upstream of, within, and downstream of the patch: $x = -0.25, -0.05,$
197 $0.05, 0.25, 0.5, 0.75, 0.95, 1.05$ and 1.25 m (Fig. 1b). For analysis, a 0.02 m-thick section was
198 sliced from the top of each core, and this was sliced in half, to enable measurements of pore
199 water in two layers (0-0.01 m and 0.01-0.02 m). This approach followed that of Reimers et al.'s
200 (2004) in situ measurements of iodide in sediments with similar grain size. The layers were
201 defrosted and centrifuged for 2 minutes at 1000 rpm to separate the pore water from the
202 sediment. The bromide concentrations in the pore water $[\text{Br}^-]_c$ were measured using high

203 performance liquid chromatography (HPLC), and expressed, following Peralta et al. (2008), as
 204 relative bromide concentration ($[\text{Br}^-]_{\text{rel}}$, %), i.e. their ratio to $[\text{Br}^-]_t$, the bromide concentration in
 205 water column:

$$206 \quad [\text{Br}^-]_{\text{rel}} = \frac{[\text{Br}^-]_c}{[\text{Br}^-]_t} \cdot 100\% \quad (1)$$

207 Velocity measurements were made using a Vectrino Acoustic Doppler Velocimeter
 208 (ADV, Nortek AS, Rud, Norway) at the same along-flume positions at which sediment samples
 209 were taken (Fig. 1b). At each location, velocities were measured at heights z_1 to $z_n = 0.005, 0.03,$
 210 $0.07, 0.095, 0.115, 0.13, 0.15, 0.18, 0.27$ and 0.31 m. All of these measurements were made at
 211 mid channel, to minimize wall effects. At each measurement point, velocity was recorded for
 212 120 seconds at 10 Hz. The height of the deflected canopy, h , was measured for every along-
 213 flume location at which velocity was measured, using a ruler attached to the side of the flume.

214 Variations in the mean flow speed (U , m s^{-1}) were calculated separately for the regions
 215 above (U_a) and within (U_b) the seagrass canopy, as averages of the flow speed measurements at
 216 each measurement height z_i , weighted by the distance between adjacent measurement
 217 heights:

$$218 \quad U_a = \frac{1}{(H-h)} \left\{ U(z_j) \left(\frac{z_j + z_{j+1}}{2} - h \right) + \sum_{i=j+1}^{n-1} U(z_i) \left(\frac{z_i + z_{i+1}}{2} - \frac{z_{i-1} + z_i}{2} \right) + U(z_n) \left(H - \frac{z_{n-1} + z_n}{2} \right) \right\} \quad (2)$$

$$219 \quad U_b = \frac{1}{h} \left\{ U(z_1) \left(\frac{z_1 + z_2}{2} \right) + \sum_{i=2}^{j-2} U(z_i) \left(\frac{z_i + z_{i+1}}{2} - \frac{z_{i-1} + z_i}{2} \right) + U(z_{j-1}) \left(h - \frac{z_{j-2} + z_{j-1}}{2} \right) \right\} \quad (3)$$

220 where z_j is the first measurement point above the top of the canopy and n is the total number
 221 of measurement points in the profile.

223 **Results**

224 **Hydrodynamic flow adjustment due to the canopy** – The flow was slower inside both
225 the long and short seagrass meadows than above them (Fig. 2). Flow within the seagrass
226 canopies gradually decelerated with distance away from leading edge, implying (due to
227 conservation of mass) that flow within the canopies had a component moving upwards and out
228 of the canopies. The horizontal velocity gradient (rate of reduction of downstream flow speed)
229 was larger in the long seagrass than in the short seagrass (Fig. 3). The adjustment length (X_D)
230 over which this reduction in in-canopy speed takes place, and the mean in-canopy flow speed
231 achieved at the end of the adjustment (U_1) are predicted by Chen et al. (2013), for canopies of
232 rigid obstacles, to be given by

233

234
$$X_D = \frac{3(1-\phi)}{C_D a} (1 + 2.3C_D a h) \quad (4)$$

235
$$U_1 = \frac{U}{1 - \frac{h}{H}\phi + \sqrt{\frac{C_D a h}{2C(1-\phi)} \left(\frac{H-h}{H}\right)^3}} \quad (5)$$

236 where ϕ is the canopy solid volume fraction, C_D the canopy drag coefficient, a the frontal area
237 per canopy volume, and $C = K_c (\delta_e/H)^{1/3}$, where K_c is an empirical coefficient which Chen et al.
238 (2013) find to be 0.07 ± 0.02 (here, we use 0.07) and δ_e is the penetration length scale of
239 vortices in the overflow into the top of the canopy, which we calculate (following Nepf et al.
240 2007) as $0.23/C_D a$. The leaf mimics used in the present experiments had widths of ~ 0.0001 m,
241 which implies solid volume fractions of $\phi = 0.0018$ for the short-leaved canopy and $\phi = 0.0048$
242 for the long-leaved canopy. There is uncertainty, however, about the appropriate values of C_D

243 for our canopies. Tanino and Nepf (2008) have investigated C_D for arrays of solid cylinders, and
244 numerous studies have reported values of C_D for a wide range of – mainly terrestrial – flexible
245 vegetation (see e.g. Wu et al., 1999), but drag coefficient values for seagrass canopies are not
246 well known, and are likely to be highly dependent on canopy structure (Peterson et al., 2004).
247 We therefore use our data and Chen et al.'s equations to back calculate values for C_D for our
248 canopies. Doing this give values of $C_D = 1.5$ for the long-leaved canopy, and $C_D = 2.1$ for the
249 short-leaved canopy. Using these values in (4) and (5) gives $X_D = 0.64$ m and $U_1 = 0.027$ ms⁻¹ for
250 the short-leaved canopy, and $X_D = 0.66$ m and $U_1 = 0.031$ ms⁻¹ for the long-leaved canopy. These
251 provide a predicted velocity decay that fits our data in the long-leaved case reasonably well, but
252 in the short-leaved case, our data shows more of a linear decay in in-canopy flow speed (Figure
253 3) rather than the exponential decay assumed by Chen et al. and observed elsewhere for arrays
254 of rigid obstacles (e.g. Belcher et al. 2003).

255 **Bromide penetration in the pore-water** – Despite the large degree of variation in the
256 data, Figure 4 shows that the relative bromide concentration $[Br^-]_{rel}$ was highest around the
257 leading edge of canopy in both depth layers in both the short- (Figure 4a) and long-leaved
258 (Figure 4b) canopies. The horizontal distance over which the solute is predicted to be able to
259 travel through the substrate in the 24 hours for which the experiment was run can be predicted
260 from the infiltration speed. This can be calculated, following Nepf and Koch (1999), as

261
$$V_D = \frac{KU^2}{gd} \tag{6}$$

262 where K is the sediment permeability (1.6×10^{-11} m²), and d , the distance over which the flow
263 deceleration at the front end of the canopy, is taken (from Figure 3) to be approximately the

264 mean value of X_D , 0.65 m. This gives $V_D = 2.22 \times 10^{-6} \text{ m s}^{-1}$, which over 24 hours gives a horizontal
265 penetration distance of 0.19 m, which is of the same order of magnitude as the length over
266 which the maximum levels of measured bromide concentration in the substrate are sustained,
267 in both of the canopies at both depths.

268 The rate at which the bromide infiltrates into the substrate can be compared to the rate
269 of uptake of nutrients by seagrasses. The value of V_D calculated above implies a volumetric rate
270 of water infiltration of $2.94 \times 10^{-6} \text{ m}^3 \text{ s}^{-1}$ per m^2 of bed surface area. If we assume that the
271 concentration of dissolved, bioavailable nitrogen in coastal waters is 0.00005-0.0005 g l^{-1} (Cozzi
272 and Giani, 2007), this would imply $0.00053\text{--}0.0053 \times 10^{-3} \text{ kg N (m}^2 \text{ sediment surface)}^{-1} \text{ hr}^{-1}$ of
273 dissolved nitrogen exchange between the water column and sediment. Rates of nitrogen
274 uptake by seagrasses vary greatly but a typical value is $5 \text{ } \mu\text{mol (g dry weight)}^{-1} \text{ hr}^{-1}$ i.e. $70 \text{ } \mu\text{g N}$
275 $(\text{g dry weight})^{-1} \text{ hr}^{-1}$ (e.g. Vonk et al., 2008). Touchette and Burkholder (2000) give a range of 5-
276 $270 \text{ } \mu\text{g N (g dry weight)}^{-1} \text{ hr}^{-1}$ for ammonium uptake. If the density of real seagrass is estimated
277 as 910 kg m^{-3} (e.g. Folkard, 2005), then the short-leaved canopy used here represents a dry
278 weight seagrass mass of $0.13 \text{ kg (m}^2 \text{ sediment bed surface area)}^{-1}$, and the long-leaved canopy
279 $0.325 \text{ kg (m}^2 \text{ sediment bed surface area)}^{-1}$. This implies that the solute exchange rate can be
280 written as $4.1\text{--}41 \text{ } \mu\text{g N (g dry weight)}^{-1} \text{ hr}^{-1}$ for the short-leaved seagrass, and $1.6\text{--}16 \text{ } \mu\text{g N (g dry}$
281 $\text{weight)}^{-1} \text{ hr}^{-1}$ for the long-leaved seagrass. These values are the same order of magnitude as
282 typical range of uptake rates of nitrogen by seagrasses, if arguably towards the lower end of
283 that range.

284

285 **Discussion**

286 **Effect of the seagrass canopy on hydrodynamics** – Our experiments demonstrate the
287 well-established pattern of flow adjustment at the upstream end of a submerged vegetation
288 canopy (e.g. Folkard, 2005; Tanino and Nepf, 2008; Chen et al., 2013), whereby part of the flow
289 travels at accelerated speeds over the top of the canopy, and part travels at decelerated speeds
290 through the canopy. They also indicate the third element of flow that we theorize above - the
291 enhancement of infiltration from the open water into the substrate while the in-canopy flow
292 decelerates as a result of the presence of the canopy. This flow is negligible in terms of water
293 discharge (in these experiments, its velocity scale is $\sim 10^{-6} \text{ ms}^{-1}$, compared to $\sim 10^{-2} \text{ ms}^{-1}$ for the
294 canopy through-flow and $\sim 10^{-1} \text{ ms}^{-1}$ for the overflow) but, as discussed below, important for
295 nutrient budgets.

296 The magnitude of the reduction in flow speed observed in both the long- and short-
297 leaved cases here is in good agreement with the predictions of Chen et al. (2013), which are
298 derived from a two-layer flow model of flows through arrays of rigid obstacles (c.f. the flexible
299 obstacles used here). This model assumes that the layers are connected via turbulent stresses
300 in the shear zone at the top of the canopy which are assumed to scale on the square of the
301 velocity difference between the layers and the length scale of the vortices within the shear
302 zone. The latter, in turn, are assumed to scale on the reciprocal of the product of the canopy
303 drag coefficient (C_D) and frontal area per unit volume (a). The adjustment length measured in
304 these experiments, over which this reduction in flow speed (X_D) occurs, fits well the predictions
305 of Chen et al. (2013) for our long-leaved canopy (Figure 5b), but appears to be slower, and
306 more linear rather than exponential, in our short-leaved canopy. Reasons for this are unclear;
307 one possibility is that relatively sparse canopies of flexible obstacles allow preferential flow

308 paths to be set up that lead to a more gradual flow decay rate at the start of the canopy (where
309 the flow is faster and more able to deflect the obstacles). But this is purely speculative, and the
310 distinction between flow decay in canopies of rigid and flexible obstacles suggested by our data
311 requires further investigation.

312 **Effects of hydrodynamic adjustment to the seagrass canopy on solute exchange** – The
313 horizontal length scale over which the highest levels of bromide concentration within the
314 sediment cores persists into the canopy (~0.2 m) matches well that predicted from the
315 assumption that the solute exchange between the open water and the substrate results from
316 the infiltration of the flow into the substrate due to its deceleration by the canopy. This
317 supports the hypothesis that the enhanced solute exchange is due to increased flow infiltration
318 as a result of the deceleration of the in-canopy flow. The lack of distinction between the
319 bromide concentrations in the 0-0.001 m and 0.001-0.002 m depth cores indicates that the
320 infiltrating water spreads more deeply than these depths. In the present study, we
321 concentrated on the horizontal extent of nutrient delivery to the substrate. The relationship
322 between the depth of infiltration and the depth of seagrass roots is also likely to be important
323 for determining seagrasses' nutrient uptake rates, and requires further investigation. The
324 variability in measured bromide concentrations (Figure 4) is quite high, and as a result there is
325 no clear difference in them between the short- and long-leaved cases studied here.

326 **Effects of solute exchange on seagrass canopy** – The fact that our estimates of nutrient
327 exchange rate are in the same range of orders of magnitude as the rate of nutrient uptake by
328 seagrasses indicates that nutrient exchange between the open water and sediment at seagrass
329 canopy edges is an important process for determining seagrass nutrient uptake in these

330 regions. Seagrasses can take up dissolved nutrients from both pore water and open water
331 (Stapel et al., 1997, Hemminga et al., 1999), but pore water nutrient concentrations are
332 generally higher (Okubo et al., 2002; Larned et al., 2004), especially in the oligotrophic waters
333 typically found in tropical seagrass environments. This implies that pore water nutrient
334 concentrations, and thus the rates of infiltration of water into the sediment are an important
335 determinant of seagrass growth rates at the upstream edges of seagrass canopies. By
336 extension, one can hypothesize that there is likely to be exfiltration of relatively nutrient-rich
337 interstitial water from the sediment into the water column at the downstream end of canopies,
338 where the near-bed open water pressure is reduced. This, therefore, is likely to be an important
339 mechanism for replenishment of nutrients in the open water. We conclude from this study that
340 the nutrient transfer rate from the open water to the pore water is determined primarily by the
341 infiltration of the flow into the substrate due to its deceleration by the canopy – as well as the
342 ambient nutrient concentration (Nishihara and Ackerman, 2006), which we have not considered
343 here. This has the effect of causing pore water dissolved nutrient concentrations to decrease
344 with increasing distance from seagrass canopy edges (over a distance of ~0.5-1 m in our study).
345 This finding has important ecological implications, as it implies favorable nutrient conditions for
346 clonal expansion at the edges of seagrass patches, which can increase the seagrass growth rate
347 and thus facilitate patch and meadow expansion. However, this also raises the question of how
348 nutrients can be delivered to pore water in the interior of seagrass meadows, where our results
349 suggest nutrient concentrations would be very low if they were purely determined by the
350 mechanism we have identified as being important here, as there is no flow deceleration here.

351 Future studies are therefore required to identify the mechanisms that ensure sufficient nutrient
352 supply to seagrasses in the interior of seagrass meadows.

353

354

355 **REFERENCES**

356

357 Apostolaki, E., Holmer, M., Marba, N., Karakassis, I. (2010). Degrading seagrass (*Posidonia*
358 *oceanica*) ecosystems: a source of dissolved matter in the Mediterranean. *Hydrobiologia* 649:
359 13-23

360

361 Barron, C., Middelburg, J.J., Duarte, C.M. (2006). Phytoplankton trapped within seagrass
362 (*Posidonia oceanica*) sediments are a nitrogen source: An in situ isotope labeling experiment.
363 *Limnol. Oceanogr.* 51: 1648–1653

364

365 Barry, S. C., Frazer, T. K., Jacoby, C. A. (2013). Production and carbonate dynamics of *Halimeda*
366 *incrassate* (Ellis) Lamouroux altered by *Thalassia testudinum* Banks and Soland ex Konig. *Jour.*
367 *Exp. Mar. Bio. Ecol.* 444: 73-80

368

369 Belcher, S.E., Jerram, N., and Hunt, J.C.R. (2003) Adjustment of a turbulent boundary layer to a
370 canopy of roughness elements. *J. Fluid Mech.* 488: 369-398

371

372 Bouma, T. J., Friedrichs, M., Klaassen, P., van Wesenbeeck, B. K., Brun, F. G., Temmerman, S.,
373 van Katwijk, M. M., Graf, G., Herman, P. M. J. (2009). Effects of shoot stiffness, shoot size and
374 current velocity on scouring sediment from around seedlings and propagules. *Mar. Ecol. Prog.*
375 *Ser.* 388: 293-297

376

377 Cambridge, M.L., Chiffings, A.W., Brittan, C., Moore, L., McComb, A.J. (1986). The loss of
378 seagrass in cockburn sound, western Australia II. possible causes of seagrass decline. *Aquatic*
379 *Bot.* 24: 269-285

380

381 Carr, J., P. D’Odorico, K. McGlathery, and P. Wiberg. (2010). Stability and bistability of seagrass
382 ecosystems in shallow coastal lagoons: role of feedbacks with sediment resuspension and light
383 attenuation. *Journal of Geophysical Research* 115: G03011. doi:10.1029/2009JG001103

384

385 Chen, Z., Jiang, C., and Nepf, H.M. (2013) Flow adjustment at the leading edge of a submerged
386 aquatic canopy. *Water Resour. Res.*, 49: 5537-5551

387

388 Christiansen M.J.A., van Belzen J., Herman P.M.J., van Katwijk M.M., Lamers L.P.M., van Leent
389 P.J.M., Bouma T.J. (2013). Low-Canopy Seagrass Beds Still Provide Important Coastal Protection
390 Services. *PLoS ONE* 8(5): e62413. doi:10.1371/journal.pone.0062413

391

392 Cozzi, S., and Giani, M. (2007) Determination of Organic Nitrogen and Urea, in L.M.L. Nollet and
393 L.S.P. de Gelder (eds.) *Handbook of Water Analysis* 2nd edition. London: CRC Press

394

395 Cullen-Unsworth, L. C., Nordlund, L. M., Paddock, J., Baker, S., McKenzie, L. J., Unsworth, R. K. F.
396 (2013). Seagrass meadows globally as a coupled social–ecological system: Implications for
397 human wellbeing. *Marine Pollution Bulletin*, 83 (2): 387-397

398

399 Duarte, C.M., Kennedy, H., Marba, N. and Hendricks, I.E. (2011) Assessing the capacity of
400 seagrass meadows for carbon burial: Current limitations and future strategies. *Ocean Coast.*
401 *Manage.* 51: 671-688
402

403 Evrard, V., Kiswara, W., Bouma, T. J., Middelburg, J. J. (2005). Nutrient dynamics of seagrass
404 ecosystems: ¹⁵N evidence for the importance of particulate organic matter and root systems.
405 *Mar. Ecol. Prog. Ser.* 295: 49-55
406

407 Finkner, S.C. and Gilley J.E. (1986). Sediment and dye concentration effects on fluorescence.
408 *Appl. Eng. Agri.* 2: 104-107
409

410 Folkard, A.M. (2005). Hydrodynamics of model *Posidonia Oceanica* patches in shallow water.
411 *Limnol. Oceanogr.* 50 (5): 1592-1600
412

413 Foster, S., Glud, R.N., Gundersen, J.K., Huettel, M. (1999) In situ study of bromide tracer and
414 oxygen flux in coastal sediments. *Est. Coast. Shelf Sci.* 49: 813-827
415

416 Gacia, E. and Duarte, C.M. (2001). Sediment retention by a mediterranean *Posidonia oceanica*
417 Meadow: The Balance between Deposition and Resuspension. *Estuar. Coast. Shelf Sci.* 52: 505-
418 514
419

420 Gilley, J.E., Finkner, S.C., Doran, J.W., Kottwitz E.R. (1990). Adsorption of bromide Tracers onto
421 sediment. *Appl. Eng. In Agri.* 6: 35-38
422

423 Glud, R.N., Gundersen, J.K., Jorgensen, B.B., Revsbech, N.P., Schulz, H.D. (1994). Diffusive and
424 total oxygen uptake of deep sea sediments in the eastern south Atlantic Ocean: in situ and
425 laboratory measurements. *Deep Sea Res.* 41: 1767-1788
426

427 Hemminga, M.A. and Marba, N. and Stapel, J. (1999). Leaf nutrient resorption, leaf lifespan and
428 the retention of nutrients in seagrass systems. *Aquatic Botany*, 65: 141-158
429

430 Hendricks, I.E., Sintes, T., Bouma, T. and Duarte, C.M. (2007). Experimental assessment and
431 modeling evaluation of the effects of seagrass (*P. oceanica*) on flow and particle trapping. *Mar.*
432 *Ecol. Prog. Ser.* 356: 163-173
433

434 Huettel, M., Gust, G. (1992). Solute release mechanisms from confined sediment cores in
435 stirred benthic chambers and flume flows. *Mar. Ecol. Prog. Ser.* 82: 187-197
436

437 Huettel, M and Rusch, A. (2000). Transport and degradation of phytoplankton in permeable
438 sediment. *Limnol. Oceanogr.* 45 (3): 534-549
439

440 Huettel, M. and Webster I. T. (2001). Porewater flow in permeable sediments. *In* Boudreau, B.P.
441 and Jorgensen, B.B [eds.], *The benthic boundary layer*. New York: Oxford Univ. Press, pp. 144-
442 179

443 Huettel, M., Ziebis, W., Forster, S., Luther III, G. W. (1998). Advective transport affecting metal
444 and nutrient distributions and interfacial fluxes in permeable sediments. *Geochimica et*
445 *Cosmochimica Acta*, 62 (4): 613-631
446

447 Kennedy, H., Beggins, J., Duarte, C. M., Fourqurean, J. W., Holmer, M., Marbà, N., and
448 Middelburg, J. J. (2010). Seagrass sediments as a global carbon sink: Isotopic constraints. *Global*
449 *Biogeochemical Cycles*, 24, GB4026, doi: 10.1029/2010GB003848
450

451 Kristensen, E., Penha-Lopes, G., Delefosse, M., Valdemarsen, T., Quintana, C.O., Banta, G.T.
452 (2012) What is bioturbation? The need for a precise definition for fauna in aquatic sciences.
453 *Mar. Ecol. Prog. Ser.* 446: 285-302
454

455 Larned, S. T., Nikora, V. I., Biggs, B. J. F. (2004). Mass transfer-limited nitrogen and phosphorus
456 uptake by stream periphyton: A conceptual model and experimental evidence. *Limnol.*
457 *Oceanogr.* 49: 1992–2000
458

459 Lewis, F. G. (1984). Distribution of macrobenthic crustaceans associated with *Thalassia*,
460 *Halodule* and bare sand substrate. *Mar. Ecol. Prog. Ser.* 19: 101-113
461

462 Lin, A.Y.C., Debroux, J.F., Cunningham, J.A., Reinhard, M.(2003). Comparison of Rhodamine-WT
463 and bromide in the determination of hydraulic characteristics of constructed wetlands. *Ecol. Eng.*
464 20 (1): 75-88
465

466 Madsen, O.S. (1978) Wave-induced pore pressures and effective stresses in a porous bed.
467 *Géotechnique* 28 (4): 377-393
468

469 Morris, L.J. and Virnstein, R. W. (2004). The Demise and Recovery of Seagrass in the Northern
470 Indian River Lagoon, Florida. *Estuaries* 27 (6): 915 - 922
471

472 Morris, E.P. and Peralta, G., E.P., Brun, F.G., Van Duren, L.A., Bouma, T.J., Perez-Llorens, J.L.
473 (2008). Interaction between hydrodynamics and seagrass canopy structure: Spatially explicit
474 effects on ammonium uptake rates. *Limnol Oceanogr* 53 (4): 1531-1539
475

476 Nepf H.M. and Koch, E.W. (1999). Vertical secondary flows in submersed plant-like arrays.
477 *Limnol. Oceanogr.* 44 (4): 1072–1080
478

479 Nepf, H.M. and Vivoni, E.R. (2000). Flow structure in depth limited, vegetated flow. *J Geophys.*
480 *Res.* 105: 28,547-28,557
481

482 Nepf, H.M., Ghisalberti, M., White, B., and Murphy, E. (2007), Retention time and dispersion
483 associated with submerged aquatic canopies, *Water Resour. Res.*, 43, W04422,
484 doi:10.1029/2006WR005362

485 Nishihara G.N. and Ackerman J.D. (2006). The effect of hydrodynamics on the mass transfer of
486 dissolved inorganic carbon to the freshwater macrophyte *Valissneria americana*. *Limnol.*
487 *Oceanogr.* 51 (6): 2734-2745
488

489 Okubo, A., Ackerman, J.D., Swaney, D.P. (2002). Passive diffusion in ecosystems. *In: Okubo, A.*
490 *and Levin, S. (eds.) Diffusion and Ecological Problems: New Perspectives.* New York: Springer
491 Verlag, pp 31–106
492

493 Owens, L.B., Van Keuren, R.W. and Edwards, W.M. (1985). Groundwater quality changes
494 resulting from a surface bromide application to a pasture. *Journ. Environ. Qual.* 14: 543-548
495

496 Palmer, M.A. (1988). Epibenthic predators and marine meio-fauna: separating predation,
497 disturbance and hydrodynamic effects. *Ecology* 69: 1251-1259
498

499 Paul, M., Bouma, T.J., Amos, C.L. (2012). Wave attenuation by submerged vegetation:
500 combining the effect of organism traits and tidal current. *Mar. Ecol. Prog. Ser.* 444: 31-41
501

502 Peduzzi, P., Herndl, G.J. (1991). Decomposition and significance of seagrass leaf litter
503 (*Cymodocea nodosa*) for the microbial food web in coastal waters (Gulf of Trieste, Northern
504 Adriatic Sea). *Mar. Ecol. Prog. Ser.* 71: 163-174
505

506 Peralta, G., Van Duren, L. A., Morris, E. P., Bouma, T. J. (2008). Consequences of shoot density
507 and stiffness for ecosystem engineering by benthic macrophytes in flow dominated areas: a
508 hydrodynamic flume study. *Mar. Ecol. Prog. Ser.* 368: 103-115
509

510 Peterson, C.H., Luettich Jr, R.A., Micheli, F., and Skilleter, G.A. (2004) Attenuation of water flow
511 inside seagrass canopies of differing structure. *Marine Ecology Progress Series* 268: 81-92
512

513 Precht, E., Huettel, M. (2004). Rapid wave-driven advective pore water exchange in a
514 permeable coastal sediment. *J Sea. Res.* 51: 93-107
515

516 Pujol, D. and Nepf, H. (2012). Breaker-generated turbulence in and above seagrass meadow.
517 *Continental Shelf Res.* (49): 1-9
518

519 Rasheed, M., Badran, M.I., Huettel, M. (2003). Influence of sediment permeability and mineral
520 composition on organic matter degradation in three sediments from the Gulf of Aqaba, Red
521 Sea. *Estuar. Coast. Shelf. Sci.* 57: 369-384
522

523 Reimers, C. E., Stecher III, H. A., Taghonb, G. L., Fuller, C. M., Huettel M., Rusch, A., Ryckelynck,
524 N., Wild, C. (2004). In situ measurements of advective solute transport in permeable shelf
525 sands. *Continental Shelf Research* 24: 183-201.
526

527 Replogle, J.A., Meyers, L.E. and Brust, K.J. (1966). Flow measurements with fluorescent tracers.
528 *ASCE J Hydraulics. Div.* 5: 1-14

529 Reyes, J. & Sansón, M. (2001). Biomass and production of the epiphytes on the
530 leaves of *Cymodocea nodosa* in the Canary Islands. *Botanica Marina* 44: 307-313
531

532 Romero, J., Lee, K. S., Perez, M., Mateo, M. A. and Alcoverro, T. (2006). Nutrient dynamics in
533 seagrass ecosystems. *In* Larkum, A.W.D., Orth, R.J. and Duarte, C.M. [eds.] *Seagrasses: biology,*
534 *ecology and conservation.* New York: Springer, pp. 227-254
535

536 Short, F.T., Polidor, B., Livingstone, S.R., Carpenter, K.E., Bandeira, S., Bujang, J.S., Calumpong,
537 H.P., Carruthers, T.J.B., Coles, R.G., Dennison, W.C., Erftemeijer, P.L.A., Fortes, M.D., Freeman,
538 A.S., Jagtap, T.G., Kamal, A.H.M., Kendrick, G.A., Kenworthy, W.J., Nafie, Y.A.L., Nasution, I.M.,
539 Orth, R.J., Prathep, A., Sanciangco, J.C., Van Tussenbroek, B., Vegara, S.G., Waycott, M., and
540 Zeiman, J.C. (2011). Extinction risk assessment of the world's seagrass species. *Biological*
541 *Conservation* 144: 1961-1971
542

543 Shum, K.T. (1992). Wave-induced advective transport below a rippled water-sediment
544 interface. *J Geophys. Res. (Oceans)* 97: 789-808
545

546 Smith, S.J. and Davis, R.J. (1974). Relative movement of bromide and nitrate through soils.
547 *Journ. Environ. Qual.* 3: 152-155
548

549 Stapel, J., Aarts, T.L., van Duynhoven, B.H.M., de Groot, J.D., van den Hoogen, P.H.W.,
550 Hemminga, M.A. (1996). Nutrient uptake by leaves and roots of the seagrass *Thalassia*
551 *hemprichii* in the Spermonde Archipelago, Indonesia. *Mar. Eco. Prog. Ser.* 134: 195-206
552

553 Tanino, Y., and Nepf, H.M. (2008), Laboratory investigation of mean drag in a random array of
554 rigid, emergent cylinders, *J. Hydraul. Eng.*, 134 (1): 34–41
555

556 Thomas, F. I. M., Cornelisen, C. D. and Zande, J. M. (2000). Effects of water velocity and canopy
557 morphology on ammonium uptake by seagrass communities. *Ecology* 81: 2704 – 2713.
558

559 Tomasko, D. A., Lapointe, B. E. (1991). Productivity and biomass of *Thalassia testudinum* as
560 related to water column nutrient availability and epiphyte levels: field observations and
561 experimental studies. *Mar. Ecol. Prog. Ser.* 75: 9-17
562

563 Touchette, B.W., and Burkholder, J.M. (2000) Review of nitrogen and phosphorus metabolism
564 in seagrasses. *J. Exp. Mar. Biol. Ecol.* 250: 133–167
565

566 Van der Heide, T., Bouma, T.J., Van Nes, E.H., Van de Koppel, J., Scheffer, M., Roelofs, J.G.M.,
567 Van Katwijk, M.M., Smolders, A.J.P. (2007). Positive feedbacks in seagrass ecosystems:
568 implications for success in conservation and restoration. *Ecosystems* 10: 1311-1322
569

570 Van Engeland, T., Bouma, T. J., Morris, E. P., Brun, F. G., Peralta, G., Lara, M., Middelburg, J. J.
571 (2011). Potential uptake of dissolved organic matter by seagrasses and macroalgae. *Mar. Ecol.*
572 *Prog. Ser.* 471: 71-81

573 Verduin, J. J., Backhaus J. O. (2000) Dynamics of plant-flow interactions for the seagrass
574 *Amphibolus antarctica*: field observations and model simulations. *Estuar Coast. Shelf Sci.* 50:
575 185-204
576
577 Vonk, J. A., Middelburg, J. J., Stapel, J., Bouma, T. J. (2008). Dissolved organic nitrogen uptake
578 by seagrasses. *Limnol. Oceanogr.* 53 (2): 542-548
579
580 Waycott, M., Duarte, C.M., Carruthers, T.J.B., Orth, R.J., Dennison, W.C., Olyarnik, S., Calladine,
581 A., Fourqurean, J.W., Heck Jr, K.L., Hughes, A.R., Kendrick, G.A., Kenworthy, W.J., Short, F.T.,
582 Williams, S.L. (2009). Accelerating loss of seagrasses across the globe threatens coastal
583 ecosystems. *Proc. Nat. Acad. Sci.* 106 (30): 12377-12381
584
585 Webb, J.E., and Theodor, J. (1972). Wave-induced circulation in submerged sands. *Journal of*
586 *Marine Biology Association UK* 52: 903-914
587
588 Wu, F.-C., Hsieh, W.S., and Chou, Y.-J. (1999) Variation of roughness coefficients for
589 unsubmerged and submerged vegetation. *Journal of Hydraulic Engineering* 125: 934-942
590

591 **Figure Legends**

592

593 Figure 1: a) Plan view of the racetrack flume tank at NIOZ, Yerseke; b) Plan view of the
594 simulated seagrass meadow placed in the test section of the flume, showing locations of
595 measurements of nutrient penetration.

596

597 Figure 2: Flow profiles for (a) short-leaved and (b) long-leaved seagrass canopies. Filled symbols
598 represent u profiles (normalized to u at $z = 0.3$ m). The dotted lines indicate the location of the
599 canopy where long-leaved seagrass bent to similar height as short-leaved seagrass height.

600

601 Figure 3: Downstream development of the mean flow speeds over the canopy (U_a ; clear
602 symbols) and within the canopy (U_b ; filled symbols) for (a) short-leaved and (b) long-leaved
603 seagrass canopies. The dotted line indicates the predictions of the model of Chen et al. (2013)
604 – see text for details. The thick black lines indicate the location of the seagrass canopy.

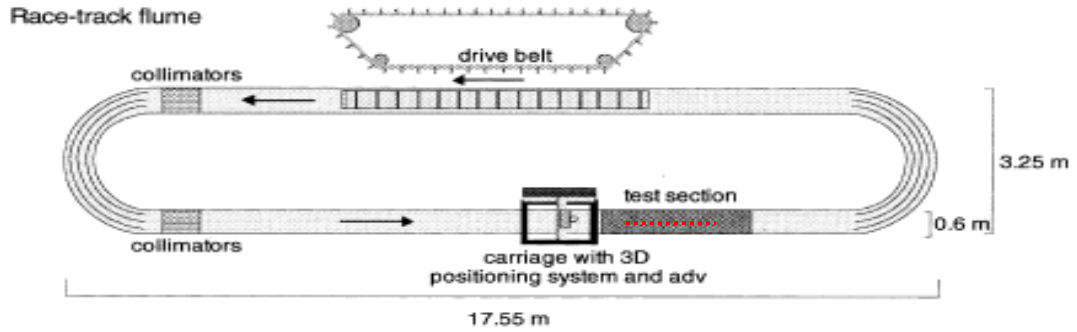
605

606 Fig. 4 Relative bromide concentration, as defined in equation (1), in the pore water measured
607 after 24 hours of running the flow, for (a) the short-leaved seagrass canopy; and (b) the long-
608 leaved seagrass canopy. Clear symbols represent relative bromide concentration in 0.01 m
609 depth; filled symbols represent relative bromide concentration in 0.02 m. Error bars show
610 standard deviation of samples measured at the three parallel locations for each x -position
611 shown in Fig. 1b.

612

613 **Figure 1**

614 **a. Race Track Flume**

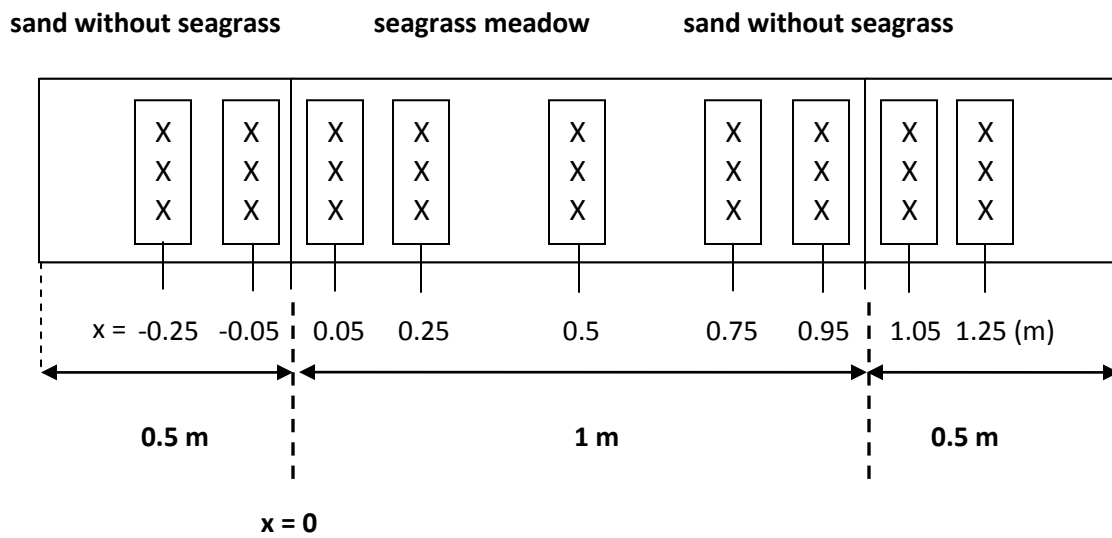


615

616 **b. Seagrass Setup and Hydrodynamic Scheme**

617

618



619

620

621

622

623

624

625

626

627

628

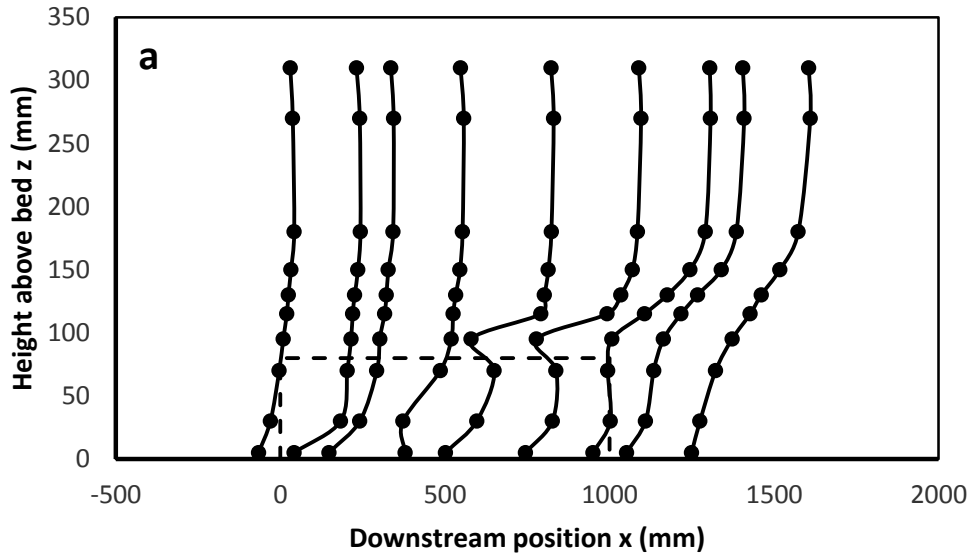
629

630

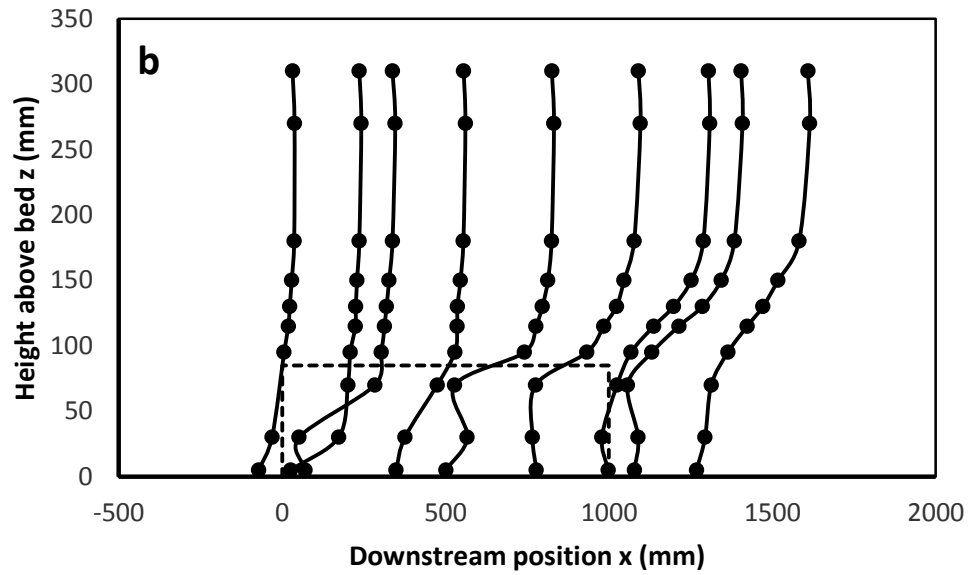
631

632 **Figure 2**

633



634



635

636

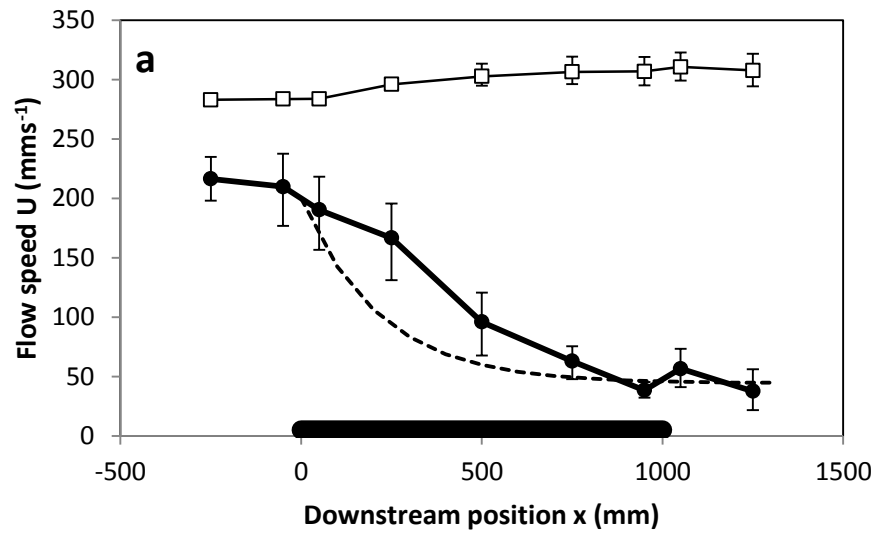
637

638

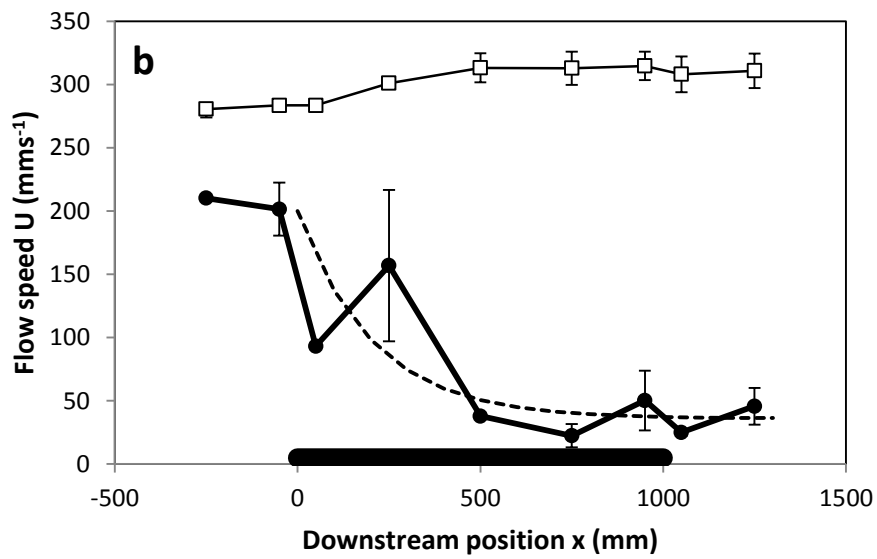
639

640 **Figure 3**

641



642

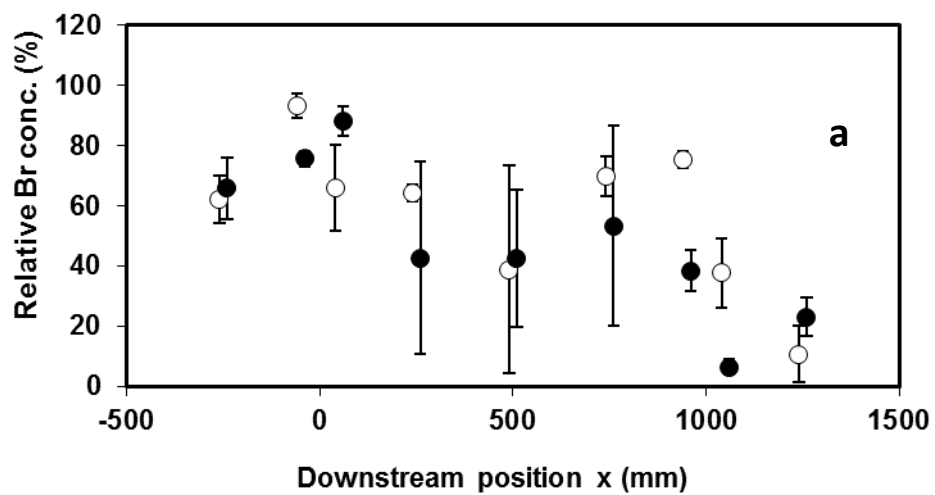


643

644

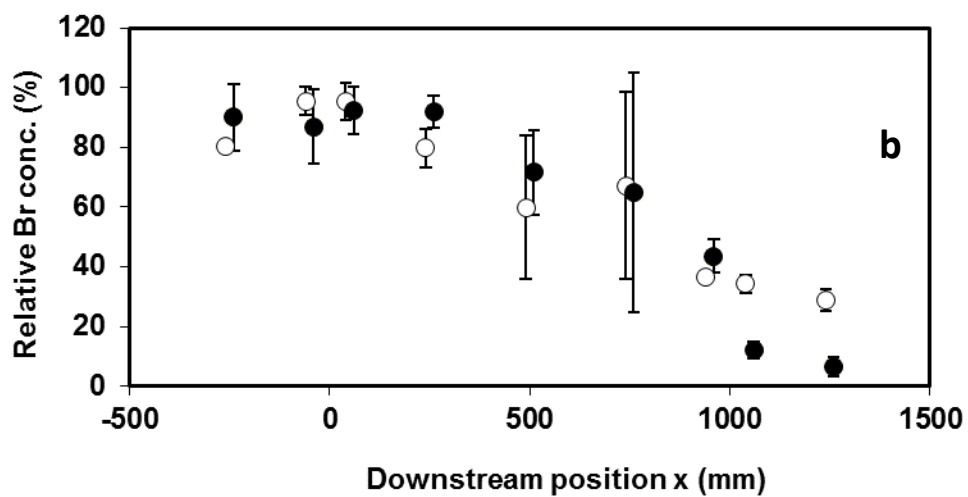
645

646 **Figure 4**



647

648



649

650

651

652

653

654

655

656